Local and Total Entropy Production and Heat and Water Fluxes in a One-Dimensional Polymer Electrolyte Fuel Cell

Signe Kjelstrup* and Audun Røsjorde

Department of Chemistry, Norwegian University of Science and Technology, N-7491 Trondheim, Norway

Received: September 9, 2004; In Final Form: February 23, 2005

We show how to determine the local entropy production rate in the various parts of a polymer electrolyte fuel cell producing liquid water from air and hydrogen. We present and solve five sets of transport equations for the heterogeneous, one-dimensional cell at stationary state, equations that are compatible with the second law of thermodynamics. The simultaneous solution of concentration, temperature, and potential profiles gave information about the local entropy production and the heat and water fluxes out of the system. Results for the entropy production can be used to explain the polarization curve, and we find that diffusion in the backing is less important for the potential than charge transport in the membrane. We demonstrate that all coupling effects as defined in nonequilibrium thermodynamics theory are essential for a correct description of the dissipation of energy and also for the small temperature gradients that were calculated here. The heat flux out of the anode was smaller than the heat flux out of the cathode. The cathode surface temperature increased as the current density increased but was smaller than the anode surface temperature for small current densities. This type of modeling may be important for design of cooling systems for fuel cells. The method is general, however, and can be used to analyze batteries and other fuel cells in a similar manner.

1. Introduction

It is well-known that the heat production in the polymer electrolyte fuel cell is large and varies with the electric current that is drawn from the cell; see Weber and Newman for a recent review on fuel cell modeling.[1] Less well-known is that the heat production may lead to temperature gradients in the cell.[2,3] Local heat production arises from irreversible and reversible processes,[4] and the temperature rise depends on the state of water in the cell as well as on local transport properties. By inclusion of nonisothermal effects in cell modeling, more knowledge may be gained on the role of the various contributions to the heat production. Information about heat fluxes, for instance, may be important for design of cell-cooling systems. The main aim of this paper is to demonstrate a physical-chemical method for calculation of the dissipated energy and the heat fluxes that accompany electrochemical processes.

A nonisothermal model for an electrochemical cell can be obtained in a systematic manner from nonequilibrium thermodynamics for heterogeneous systems. The method of description is general and can be used for other electrochemical systems. It may be particularly useful when large parts of the available electric potential is dissipated as heat. A first attempt to describe the nonisothermal polymer electrolyte fuel cells was made by Kjelstrup and co-workers,[2,6] while Janssen[5] gave a detailed, systematic analysis of the isothermal cell using this theory. In this work, we extend the earlier efforts,[5,6,7] by solving a full set of equations for all five subsystems of the nonisothermal cell.

An advantage of using nonequilibrium thermodynamics is that we obtain the possibility for consistency control. Most fuel cell models presented in the literature so far are based upon solutions of the conservation equations of mass, momentum, and electric charge, and in the modeling of nonisothermal cells, the energy balance is also included.[1] So far, the entropy production and the entropy balance have not been used actively in a description of electrochemical cells. We shall calculate the total entropy production in the cell from the entropy balance over the whole system but also by integrating over all local contributions to the entropy production inside the system. The two calculations must give the same result for a model that obeys the second law of thermodynamics. This has not been discussed previously for electrochemical cells.

The interplay between the isothermal transport processes that take place in the fuel cell has been analyzed by many authors.[1,10] It is generally acknowledged that most of the dissipation of energy in the cell is due to electrode overpotentials and ohmic resistivities. From the polarization curve, the next source of energy dissipation has often been allocated to the gas diffusion backing of the cell; see, for example, ref 8. By calculating the local entropy production rate, one can investigate the sources of dissipation. In this work, we shall see for a special case that despite having diffusion limitations in the anode there is a negligible entropy production in this location.

The present method development and calculations are also motivated by two questions: What is the temperature profile across the cell under some operating conditions, and what are the heat fluxes from the two cell walls, given the electric current density and the water flux? Such questions cannot be answered when one is not concerned with the local heat production. In studies of thermal management in electrochemical cells, so far only the whole cell performance have been considered.[1,3,9,11] For instance, the total cell potential or the total heat production has been calculated rather than the profiles in these variables across the cell. It is thus a purpose here to contribute to the understanding of energy management by adding information from the local level.

As an example cell, we have taken a polymer membrane fuel cell operating on pure hydrogen and air at 1 bar in its stationary

* Author to whom correspondence should be addressed. Phone: +47 73594179. Fax: +47 7355087. E-mail: Signe.Kjelstrup@phys.chem.ntnu.no.

10.1021/jp040608k CCC: $30.25
Published on Web 04/05/2005

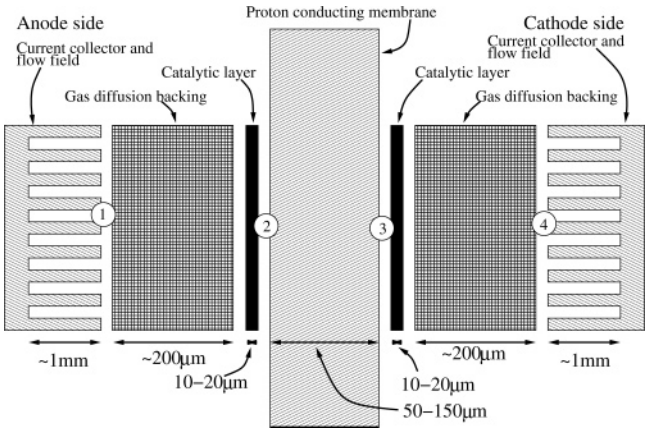

Figure 1. Five subsections of the polymer electrolyte fuel cell (for explanations, see text). Typical dimensions are indicated. Courtesy of P. Vie.

state. The membrane is a standard membrane in the literature, Nafion 115. Water is produced in its liquid form, since the temperature is approximately 70 °C. The subsystems of the cell are illustrated in Figure 1. They are the diffusion backing in the anode (between 1 and 2 in the figure), the anode surface catalytic layer (dark region at 2), the proton-conducting, water-containing membrane (between 2 and 3), the cathode surface catalytic layer (at 3), and the diffusion backing in the cathode (between 3 and 4). The uttermost layers in Figure 1 illustrate the current collector system and the gas flow channels in the cell.

2. Theory

We apply nonequilibrium thermodynamics (NET) to transport in heterogeneous materials.[6] A heterogeneous material is composed of several thermodynamic subsystems, i.e., homogeneous systems and surfaces. NET is since long-established for homogeneous systems; see, for example, ref 12. The corresponding equations for surfaces were written by Bedeaux and co-workers.[6,13−16] In the description of a heterogeneous system such as the fuel cell, where NET for homogeneous systems is combined with NET for surfaces, we proceed as follows:

- The heterogeneous fuel cell is divided into three bulk and two surface subsystems, as described above. The bulk systems are the backing materials for the electrode surfaces and the water-containing membrane of the single cell; see Figure 1. The surfaces are the anode and cathode catalytic surfaces, where the electrode reactions take place (2 and 3 in Figure 1.)
- The backing material on both sides is a porous carbon matrix for transport of heat, charge, and mass. The gas transport takes place in the pores, while the charge transport takes place in the solid part of the matrix. The fluxes are averages over the cross-sectional surface of these subsystems.
- The surfaces are described using excess variables according to Gibbs.[17] The variables are thus integrals over the thickness of the surface, which here is 10 μm. In this manner, we are able to deal with the finite thickness of a surface, a problem that has been raised in the literature.[8]
- Transport equations are derived from the entropy production rate for each subsystem. Only independent variables are used in the entropy production rate.
- The electrode surfaces are chosen as the frame of reference for the transport processes. (The results do not depend on the chosen frame of reference.)

The system's performance is given by the transport equations, which follow from the entropy production rate, the conservation equations for mass and energy, and the overall entropy balance. We give first the entropy balance for the total cell and proceed with the entropy production and the transport equations for all five subsystems in the cell. We limit ourselves to stationary state calculations and to a one-dimensional transport problem.

2.1. Total Entropy Balance and the Local Entropy Production. Consider the single polymer electrode fuel cell, with the membrane electrolyte sandwiched between the anode and cathode regions. The direction of transport is from the anode to the cathode. In a one-dimensional model of the cell, the system is adiabatic along the axis of transport. The anode surface reaction is

$$\frac{1}{2}H_2 \rightarrow H^+ + e^- \tag{1}$$

The cathode surface reaction is

$$\frac{1}{4}O_2 + H^+ + e^- \rightarrow \frac{1}{2}H_2O \tag{2}$$

The stationary state mass fluxes are given by the electric current density j

$$J_{H_2} = \frac{j}{2F}$$

$$J_{O_2} = -\frac{j}{4F} \tag{3}$$

where F is Faraday's constant. There is a constant flux of water J_w^a across the anode backing and anode surface to keep the membrane from drying out. The water flux out of the cathode surface is for reasons of continuity

$$J_w^c = J_w^a + \frac{j}{2F} \tag{4}$$

Superscript a means anode, while c means cathode. The entropy production of the whole cell per unit of membrane area and time is (Appendix A)

$$\frac{dS_{irr}}{dt} = \frac{J_q'^c}{T^{c,0}} - \frac{J_q'^a}{T^{a,0}} + \frac{j}{F}\left[\frac{1}{2}(S_w^{c,0} - S_{H_2}^{a,0}) - \frac{1}{4}S_{O_2}^{c,0}\right] + J_w^a[S_w^{c,0} - S_w^{a,0}] \tag{5}$$

where S_i is the thermodynamic entropy of i, $J_q'^a$ and $J_q'^c$ are the sensible heat fluxes, and $T^{a,0}$ and $T^{c,0}$ are the temperatures of the anode and cathode boundaries of the cell. The first superscript indicates the phase, and the second the nearest phase. The symbol 0 is used for the gas flow channels; see Figure 1. In nonequilibrium thermodynamics, the sensible heat fluxes have several terms, not only Fourier-type terms, as we shall see below. All terms are important in the development of a consistent thermodynamic model.

The value of dS_{irr}/dt is also the integral over contributions from all five subsystems

$$\frac{dS_{irr}}{dt} = \int_{a,0}^{a,m} \sigma^a \, dx + \sigma^{s,a} + \int_{m,a}^{m,c} \sigma^m \, dx + \sigma^{s,c} + \int_{c,m}^{c,0} \sigma^c \, dx \geq 0 \tag{6}$$

The superscript m stands for membrane. The excess entropy production rate in the anode and cathode surfaces (in J/(s K

m^2)) are $\sigma^{s,a}$ and $\sigma^{s,c}$. In the bulk phases, we have σ^j, with j = a, m, c (in J/(s K m^3)). The second law requires that $dS_{irr}/dt > 0$ but also that $\sigma^i > 0$ and $\sigma^{s,i} > 0$ for i = a, c.

The two expressions above must give the same answer for the total entropy production. We shall use this as a consistency criterion for our thermodynamic model. We proceed to find the simultaneous solution to the equations for the five subsections. The solutions give the concentration profiles, the temperature profile, the electric potential profile, and the heat fluxes through the cell, plus the accumulated entropy production rate. The accumulated entropy production rate (eq 6) is in the end compared to eq 5. While eq 6 is calculated from knowledge of all the local transport parameters, eq 5 is found from fluxes and functions of state. The calculations are therefore independent of one another and are useful for a consistency control.

The terminology follows de Groot and Mazur;[12] see also the Symbol list. A single superscript is used to indicate the relevant subsystem (a, m, c, or s), when a variable is relevant for several subsystems. When a double superscript is used, the first gives the subsystem, and the second gives the nearest subsystem. For instance, a,m means the anode backing close to the membrane.

2.2. Anode Backing. Consider first the transport of heat, hydrogen, water, and charge through the anode backing. The energy flux, J_u, through the backing is constant, giving

$$\frac{d}{dx}J_u = \frac{d}{dx}J'^{a}_q + j\frac{d\phi}{dx} + J_{H_2}\frac{dH_{H_2}}{dx} + J^a_w\frac{dH^a_w}{dx} = 0 \qquad (7)$$

where H_i is the partial molar enthalpy of i and $dH_i/dx = c_{p,i}dT/dx$.

We assume that hydrogen and water are transported in the pores of the anode backing at constant pressure, p^0. The transport of charge and heat takes place in the solid material of the backing. The entropy production rate for these transports is[12]

$$\sigma^a = J'^{a}_q\frac{d}{dx}\left(\frac{1}{T}\right) - J^a_w\frac{1}{T}\frac{d\mu^a_{w,T}}{dx} - J_{H_2}\frac{1}{T}\frac{d\mu_{H_2,T}}{dx} - j\frac{1}{T}\frac{d\phi}{dx} \qquad (8)$$

Here, ϕ is the electric potential, and $\mu_{i,T}$ is the chemical potential of component i differentiated at constant temperature. The fluxes of water, hydrogen, and the electric current density are constant. They refer always to the whole membrane area, even if the actual transport takes place across a smaller area, the cross-sectional area of all pores.

The chemical potential of hydrogen and water at constant temperature are related through the Gibbs−Duhem equation

$$\frac{d\mu_{H_2,T}}{dx} = -\frac{x^a_w}{x_{H_2}}\frac{d\mu^a_{w,T}}{dx} \qquad (9)$$

where x_i is the mole fraction of i. Equations 9 and 3 reduce the entropy production rate to

$$\sigma^a = J'^{a}_q\frac{d}{dx}\left(\frac{1}{T}\right) - j\frac{1}{T}\frac{d\phi}{dx} - J^a_D\frac{1}{T}\frac{d\mu^a_{w,T}}{dx} \qquad (10)$$

where the interdiffusion flux of water and hydrogen is

$$J^a_D = \left(\frac{J^a_w}{x^a_w} - \frac{J_{H_2}}{x_{H_2}}\right)x^a_w = \left(\frac{J^a_w}{x^a_w} - \frac{j}{2Fx_{H_2}}\right)x^a_w \qquad (11)$$

The dominant part of J^a_D is the last part, as $j/F \gg J^a_w$ for most conditions. The differential equations that determine the variation in the intensive variables are found from the flux equations that derive from the entropy production rate. For the anode backing, they are (for details, see Appendix B)

$$\frac{dT}{dx} = -\frac{1}{\lambda^a}\left[J'^{a}_q - q^{*,a}\left(J^a_D - t^a_D\frac{j}{F}\right) - \pi^a\frac{j}{F}\right]$$

$$\frac{dx^a_w}{dx} = -\frac{q^{*,a}x^a_w}{RT^2}\frac{dT}{dx} - \frac{J^a_D - t^a_D j/F}{D_{wH}}$$

$$\frac{d\phi}{dx} = -\frac{\pi^a}{TF}\frac{dT}{dx} - \frac{t^a_D RT}{Fx^a_w}\frac{dx^a_w}{dx} - r^a j \qquad (12)$$

There are six independent transport coefficients; all are defined in Appendix B. The main coefficients are the thermal conductivity, λ^a, the interdiffusion coefficient for water and hydrogen, D_{wH}, and the ohmic resistivity, r^a. The coupling coefficients of the system are contained in the transference coefficient t^a_D, the Peltier heat, π^a, and the heat of transfer, $q^{*,a}$. The transference coefficient, t^a_D, is defined by

$$t^a_D = F\left(\frac{J^a_D}{j}\right)_{dT=0,d\mu_w=0} = t^a_w - \frac{x^a_w}{2x_{H_2}} \qquad (13)$$

where t^a_w is the transference coefficient for water in the anode. The Peltier heat of the anode, π^a, is likewise

$$\pi^a = F\left(\frac{J'^{a}_q}{j}\right)_{dT=0,d\mu_w=0} = -T\left(\frac{1}{2}S_{H_2} + S^{*,a}_e\right) \qquad (14)$$

where $S^{*,a}_e$ is the transported entropy of electrons in the anode and the expression for S_{H_2} is further specified in the data section. In Appendix A, we obtained the following estimate for the heat of transfer of water in the anode

$$q^{*,a} = \left(\frac{J'^{a}_q}{J^a_D}\right)_{dT=0,j=0} = -TS^a_w \qquad (15)$$

All six transport coefficients are then known and can be used to solve eqs 12 together with the energy balance.

We see from eqs 12 that the temperature gradient has three contributions. When the current density is large, the last contribution is significant compared to the Fourier-type contribution and the contribution from the water flux. Likewise, there is a contribution to the gradient in the mole fraction of water from the temperature gradient, but this contribution is not significant in magnitude. The gradient in the water mole fraction in the anode is calculated from this equation. At the left-hand side of the anode, the mole fraction is $x^0_w = p^*_w/p^0$ where p^*_w is the vapor saturation pressure at $T^{a,0}$. The vapor saturation pressure is rather temperature dependent (see section 3). The partial pressure of water is calculated to find the water activity at the membrane side. It is given from x^a_w and the total pressure, $p_w = x^a_w p^0$. The electric potential gradient does not only have an ohmic contribution, $-r^a j$. For conditions used here, the other two contributions are small, but they are needed for perfect agreement between the different expressions for the entropy production, eqs 5 and 6.

2.3. Anode Catalyst Surface. At the anode catalyst surface, the enthalpy of hydrogen is converted into electric energy and heat. There is a change in the enthalpy as water goes from the vapor state to the condensed state in the membrane. This also

releases heat. Conservation of energy across the phase boundary means that

$$J_u = J'^{\mathrm{a,m}}_q + j\phi^{\mathrm{a,m}} + J_{\mathrm{H_2}} H^{\mathrm{a,m}}_{\mathrm{H_2}} + J^{\mathrm{a}}_{\mathrm{w}} H^{\mathrm{a,m}}_{\mathrm{w}} = J'^{\mathrm{m,a}}_q + j\phi^{\mathrm{m,a}} + J^{\mathrm{m}}_{\mathrm{w}} H^{\mathrm{m,a}}_{\mathrm{w}} \quad (16)$$

The flux of hydrogen stops at the surface, while the electric current density and the water flux are continuous and constant in the anode backing, through the surface and in the membrane

$$J^{\mathrm{a}}_{\mathrm{w}} = J^{\mathrm{m}}_{\mathrm{w}} \quad (17)$$

The difference in the electric potential between the two sides of the surface $\phi^{\mathrm{m,a}} - \phi^{\mathrm{a,m}} = \Delta_{\mathrm{a,m}}\phi$ is generated by the heat and enthalpy changes.

The details of the conditions at the surface are not known. To simplify the matter enough to make possible a calculation of the profiles of T, x_{w}, and ϕ across the surface and thereby across the cell, we assume that there is equilibrium for water across the surfaces between the electrode backing and the membrane. This assumption is standard in fuel cell modeling. At the anode, we then have

$$\Delta_{\mathrm{a,m}}\mu_{\mathrm{w}} = (H^{\mathrm{m,a}}_{\mathrm{w}} - T^{\mathrm{m,a}} S^{\mathrm{m,a}}_{\mathrm{w}}) - (H^{\mathrm{a,m}}_{\mathrm{w}} - T^{\mathrm{a,m}} S^{\mathrm{a,m}}_{\mathrm{w}}) = 0 \quad (18)$$

This relation can be used to find the temperature on the membrane side close to the anode, $T^{\mathrm{m,a}}$, or the temperature on the anode side close to the membrane, $T^{\mathrm{a,m}}$, from known thermodynamic properties. Enthalpies and entropies are temperature functions; see section 3. We shall also use the corresponding relation at the cathode surface. These restrictions limit the possibilities to find a numerical solution, however.

The entropy production of an electrode surface was given by Bedeaux and co-workers.[6,13−15]

$$\sigma^{\mathrm{s,a}} = J'^{\mathrm{a,m}}_q \Delta_{\mathrm{a,s}}\left(\frac{1}{T}\right) + J'^{\mathrm{m,a}}_q \Delta_{\mathrm{s,m}}\left(\frac{1}{T}\right) - J_{\mathrm{w}} \frac{1}{T^{\mathrm{s,a}}} \Delta_{\mathrm{a,m}}\mu_{\mathrm{w},T}(T^{\mathrm{s,a}}) - j\frac{1}{T^{\mathrm{s}}}\left(\Delta_{\mathrm{a,m}}\phi - \frac{\mu^{\mathrm{a,m}}_{\mathrm{H_2},T}(T^{\mathrm{s,a}})}{2F}\right) \quad (19)$$

where $T^{\mathrm{s,a}}$ is the temperature of the anode surface. There is a discontinuity in the heat flux at the surface, so we distinguish between the heat flux into the surface, $J'^{\mathrm{a,m}}_q$, and out of the surface, $J'^{\mathrm{m,a}}_q$. The subscripts a,m, a,s, and s,m mean that the difference is taken between the membrane and the anode, the surface and the anode, and the membrane and the surface, respectively. The electrochemical reaction takes place at the surface, and the reaction rate at stationary state is equal to j/F. We have also used the stationary state value for the hydrogen flux. With equilibrium for water across the surface, eq 18

$$\Delta_{\mathrm{a,m}}\mu_{\mathrm{w},T}(T^{\mathrm{s,a}}) = H^{\mathrm{m,a}}_{\mathrm{w}} - H^{\mathrm{a,m}}_{\mathrm{w}} - T^{\mathrm{s,a}}(S^{\mathrm{m,a}}_{\mathrm{w}} - S^{\mathrm{a,m}}_{\mathrm{w}}) = S^{\mathrm{a,m}}_{\mathrm{w}}(T^{\mathrm{s,a}} - T^{\mathrm{a,m}}) + S^{\mathrm{m,a}}_{\mathrm{w}}(T^{\mathrm{m,a}} - T^{\mathrm{s,a}}) \quad (20)$$

The effective electrical force is

$$\Delta_{\mathrm{a,m}}\phi_{\mathrm{eff}} = \Delta_{\mathrm{a,m}}\phi - \frac{\mu^{\mathrm{a,m}}_{\mathrm{H_2},T}(T^{\mathrm{s,a}})}{2F} \quad (21)$$

The equations of transport that derive from this $\sigma^{\mathrm{s,a}}$, given in Appendix D, are

$$\Delta_{\mathrm{a,s}}T = -\frac{1}{\lambda^{\mathrm{s}}_{\mathrm{a}}}\left[J'^{\mathrm{a,m}}_q - q^{*,\mathrm{a}}\left(J_{\mathrm{w}} - t_{\mathrm{w}}\frac{j}{F}\right) - \pi^{\mathrm{a}}\frac{j}{F}\right] \quad (22a)$$

$$\Delta_{\mathrm{a,s}}\mu_{\mathrm{w},T} = -\frac{q^{\mathrm{a},*}}{T^{\mathrm{a,m}}}\Delta_{\mathrm{a,s}}T - \frac{(J_{\mathrm{w}} - t_{\mathrm{w}}j/F)}{l^{\mathrm{s}}_{\mu\mu}} \quad (22b)$$

$$\Delta_{\mathrm{s,m}}T = -\frac{1}{\lambda^{\mathrm{s}}_{\mathrm{m}}}\left[J'^{\mathrm{m,a}}_q - q^{*,\mathrm{m}}\left(J_{\mathrm{w}} - t_{\mathrm{w}}\frac{j}{F}\right) + \pi^{\mathrm{m}}\frac{j}{F}\right] \quad (22c)$$

$$\Delta_{\mathrm{s,m}}\mu_{\mathrm{w},T} = -\frac{q^{*,\mathrm{m}}}{T^{\mathrm{m,a}}}\Delta_{\mathrm{s,m}}T - \frac{(J_{\mathrm{w}} - t_{\mathrm{w}}j/F)}{l^{\mathrm{s}}_{\mu\mu}} \quad (22d)$$

$$\Delta_{\mathrm{a,m}}\phi_{\mathrm{eff}} = -\frac{\pi^{\mathrm{a}}}{T^{\mathrm{a,m}}F}\Delta_{\mathrm{a,s}}T - \frac{\pi^{\mathrm{m}}}{T^{\mathrm{m,a}}F}\Delta_{\mathrm{s,m}}T - \frac{t_{\mathrm{w}}}{F}\Delta_{\mathrm{a,m}}\mu_{\mathrm{w},T} - r^{\mathrm{s}}j \quad (22e)$$

The heat fluxes have a Fourier-type contribution as well as a contribution from the Peltier heat and the heat of transfer according to NET. There are changes in $\mu_{\mathrm{w},T}$ from the fluxes of water or charge and from the temperature jumps. The electric potential drop at the surface has contributions from the Peltier coefficients, the chemical potential differences, and the resistance drop across the surface. We have neglected the overpotential in this electrode.

These equations, together with the energy balance and eq 18, can be solved for the temperature jumps and the electric potential drop at the surface. The Peltier coefficients are known, while the thermal and mass conductivities are not. Condition eq 18 was therefore used instead of the equation for the equations that give the jumps in chemical potential. When the heat flux in the anode backing is known from section 2.2, the heat flux in the membrane can be found from the energy balance.

2.4. Membrane. Energy conservation in the membrane means that

$$\frac{\mathrm{d}}{\mathrm{d}x}J_u = \frac{\mathrm{d}}{\mathrm{d}x}(J'^{\mathrm{m}}_q + j\phi^{\mathrm{m}} + J^{\mathrm{m}}_{\mathrm{w}} H^{\mathrm{m}}_{\mathrm{w}}) = 0 \quad (23)$$

The equation gives the connection between the gradient in electric potential across the membrane and the change in the heat flux in the membrane, which in turn will affect the heat fluxes out of the electrode backings. The entropy production rate has again three terms

$$\sigma = J'^{\mathrm{m}}_q \frac{\mathrm{d}}{\mathrm{d}x}\left(\frac{1}{T}\right) - j\frac{1}{T}\frac{\mathrm{d}\phi}{\mathrm{d}x} - J^{\mathrm{m}}_{\mathrm{w}}\frac{1}{T}\frac{\mathrm{d}\mu^{\mathrm{m}}_{\mathrm{w},T}}{\mathrm{d}x} \quad (24)$$

The derivation of the flux equation that follows from this expression is given in Appendix C. In the membrane, water is not in an ideal state, but its activity a_{w} is known as a function of the water content λ[18] (in moles of water per mole of membrane ionic sites). The differential equations become

$$\frac{\mathrm{d}T}{\mathrm{d}x} = -\frac{J'^{\mathrm{m}}_q}{\lambda^{\mathrm{m}}} + \frac{q^{*,\mathrm{m}}}{\lambda^{\mathrm{m}}}\left(J^{\mathrm{m}}_{\mathrm{w}} - t^{\mathrm{m}}_{\mathrm{w}}\frac{j}{F}\right) + \frac{\pi^{\mathrm{m}}j}{F\lambda^{\mathrm{m}}}$$

$$\frac{\mathrm{d}a_{\mathrm{w}}}{\mathrm{d}x} = -\frac{q^{*,\mathrm{m}}\lambda}{(\mathrm{d}\lambda/\mathrm{d}a_{\mathrm{w}})RT^2}\frac{\mathrm{d}T}{\mathrm{d}x} - \frac{(J^{\mathrm{m}}_{\mathrm{w}} - t^{\mathrm{m}}_{\mathrm{w}}j/F)M}{(\mathrm{d}\lambda/\mathrm{d}a_{\mathrm{w}})\rho D^{\mathrm{m}}_{\mathrm{w}}}$$

$$\frac{\mathrm{d}\phi}{\mathrm{d}x} = -\frac{\pi^{\mathrm{m}}}{TF}\frac{\mathrm{d}T}{\mathrm{d}x} - \frac{t_{\mathrm{w}}{}^{\mathrm{m}}RT}{Fa_{\mathrm{w}}}\frac{\mathrm{d}a_{\mathrm{w}}}{\mathrm{d}x} - r^{\mathrm{m}}j \quad (25)$$

The membrane dry density is ρ, and the molar mass of the Nafion polymer is M. The Peltier coefficient for the membrane is τ^{m}. The expression for the heat of transfer $q^{*,\mathrm{m}}$ is chosen similar to the expression for the anode. The heat production in the membrane and at its surfaces is central, and we shall use two models for the electric resitivity, r^{m}. The most complicated one was taken from Springer et al.[18]

$$(r^{\mathrm{m}})^{-1} = \exp\left(1268\left(\frac{1}{303} - \frac{1}{T}\right)\right)(0.5139\lambda - 0.326) \quad (26)$$

Alternatively, we neglected the temperature and water-content variation in r^{m}. The value for $\lambda = 1$ was used, when the water content was smaller than this value (but larger than zero). We solve first the temperature gradient from the first of the equations and proceed to find the gradient in water content and the electric potential gradient from the following.

2.5. Cathode Catalyst Surface. Energy conservation at the cathode surface gives

$$J_{\mathrm{u}} = J'^{\mathrm{m,c}}_q + j\phi^{\mathrm{m,c}} + J^{\mathrm{m}}_{\mathrm{w}} H^{\mathrm{m,c}}_{\mathrm{w}} = J'^{\mathrm{c,m}}_q + j\phi^{\mathrm{c,m}} + (J^{\mathrm{m}}_{\mathrm{w}} + j/2F)H^{\mathrm{c,m}}_{\mathrm{w}} + J_{\mathrm{O_2}} H^{\mathrm{c,m}}_{\mathrm{O_2}} \quad (27)$$

where we used $J^{\mathrm{c}}_{\mathrm{w}} = J^{\mathrm{m}}_{\mathrm{w}} + j/2F$. The equation for the entropy production rate of the cathode surface is similar to the equation for the anode; see subsection 2.3. The potential jump across the surface is $\Delta_{\mathrm{m,c}}\phi = \phi^{\mathrm{c,m}} - \phi^{\mathrm{m,c}}$. The effective electrical force is

$$\Delta_{\mathrm{m,c}}\phi_{\mathrm{eff}} = \Delta_{\mathrm{m,c}}\phi - \frac{\mu^{\mathrm{c,m}}_{\mathrm{O_2},T}(T^{\mathrm{s,c}})}{4F} + \frac{\mu^{\mathrm{c,m}}_{\mathrm{w},T}(T^{\mathrm{s,c}})}{2F} \quad (28)$$

Equations to be solved for the profiles are then

$$\Delta_{\mathrm{m,s}}T = -\frac{1}{\lambda^{\mathrm{s}}_{\mathrm{m}}}\left[J'^{\mathrm{m,c}}_q - q^{*,\mathrm{m}}\left(J^{\mathrm{m}}_{\mathrm{w}} - t^{\mathrm{m}}_{\mathrm{w}}\frac{j}{F}\right) - \pi^{\mathrm{m}}\frac{j}{F}\right] \quad (29a)$$

$$\Delta_{\mathrm{m,s}}\mu_{\mathrm{w},T} = -\frac{q^{*,\mathrm{m}}}{T^{\mathrm{m,c}}}\Delta_{\mathrm{m,s}}T - \frac{(J^{\mathrm{m}}_{\mathrm{w}} - t^{\mathrm{m}}_{\mathrm{w}}j/F)}{l^{\mathrm{s}}_{\mu\mu}} \quad (29b)$$

$$\Delta_{\mathrm{s,c}}T = -\frac{1}{\lambda^{\mathrm{s}}_{\mathrm{c}}}\left[J'^{\mathrm{c,m}}_q - q^{*,\mathrm{c}}\left(J^{\mathrm{c}}_{\mathrm{w}} - t^{\mathrm{c}}_{\mathrm{w}}\frac{j}{F}\right) - \pi^{\mathrm{c}}\frac{j}{F}\right] \quad (29c)$$

$$\Delta_{\mathrm{s,c}}\mu_{\mathrm{w},T} = -\frac{q^{*,\mathrm{c}}}{T^{\mathrm{c,m}}}\Delta_{\mathrm{s,c}}T - \frac{(J^{\mathrm{c}}_{\mathrm{w}} - t^{\mathrm{c}}_{\mathrm{w}}j/F)}{l^{\mathrm{s}}_{\mu\mu}} \quad (29d)$$

$$\Delta_{\mathrm{m,c}}\phi_{\mathrm{eff}} + \eta^{\mathrm{c}} = -\frac{\pi^{\mathrm{m}}}{FT^{\mathrm{m}}}\Delta_{\mathrm{m,s}}T - \frac{\pi^{\mathrm{c}}}{FT^{\mathrm{c}}}\Delta_{\mathrm{s,c}}T - \frac{t^{\mathrm{m}}_{\mathrm{w}}\Delta_{\mathrm{m,s}}\mu_{\mathrm{w},T}}{F} - \frac{t^{\mathrm{c}}_{\mathrm{w}}\Delta_{\mathrm{s,c}}\mu_{\mathrm{w},T}}{F} - r^{\mathrm{s}}j \quad (29e)$$

Only the first, third, and fifth equations were used to solve the temperature and the electric potential profile. The equations for the change in the chemical potential of water were not used, since we preferred to use the condition for equilibrium for water across the surface; cf. eq 18. The effective electrical force is reduced by the overpotential of the oxygen electrode, η^{c}. The overpotentential is the excess potential needed to overcome the resistance of the chemical reaction at a given current density j. Rubi and Kjelstrup[19] showed that the overpotential plus the electric potential drop was the effective driving force for charge transfer in isothermal systems. The overpotential has not yet been defined for a nonisothermal electrode. In the absence of such a definition, we assumed eq 29e.

2.6. Cathode Backing. Energy conservation in the cathode backing means that

$$\frac{\mathrm{d}}{\mathrm{d}x}J_{\mathrm{u}} = \frac{\mathrm{d}}{\mathrm{d}x}(J'^{\mathrm{c}}_q + j\phi^{\mathrm{c}} + J^{\mathrm{c}}_{\mathrm{w}} H^{\mathrm{c}}_{\mathrm{w}} + J_{\mathrm{N_2}}H^{\mathrm{c}}_{\mathrm{N_2}} + J_{\mathrm{O_2}}H^{\mathrm{c}}_{\mathrm{O_2}}) = 0 \quad (30)$$

where we again use that $\mathrm{d}H_{\mathrm{i}}/\mathrm{d}x = c_{\mathrm{p,i}}\mathrm{d}T/\mathrm{d}x$. Oxygen is available from air, so there is also nitrogen in the cathode, but $J_{\mathrm{N_2}} = 0$ in the surface frame of reference. Relations between the component fluxes and the electric current were given in section 2.1.

The entropy production rate is

$$\sigma^{\mathrm{c}} = J'^{\mathrm{c}}_q\frac{\mathrm{d}}{\mathrm{d}x}\left(\frac{1}{T}\right) - J^{\mathrm{c}}_{\mathrm{w}}\frac{1}{T}\frac{\mathrm{d}\mu_{\mathrm{w},T}}{\mathrm{d}x} - J_{\mathrm{O_2}}\frac{1}{T}\frac{\mathrm{d}\mu_{\mathrm{O_2},T}}{\mathrm{d}x} - J_{\mathrm{N_2}}\frac{1}{T}\frac{\mathrm{d}\mu_{\mathrm{N_2},T}}{\mathrm{d}x} - j\frac{1}{T}\frac{\mathrm{d}\phi}{\mathrm{d}x} \quad (31)$$

A flux of water is maintained, countering the flux of oxygen. The three gases distribute themselves and keep the pressure constant. By introducing the relationship between the chemical potential gradients

$$\frac{\mathrm{d}\mu_{\mathrm{O_2},T}}{\mathrm{d}x} = -\frac{x^{\mathrm{c}}_{\mathrm{w}}}{x_{\mathrm{O_2}}}\frac{\mathrm{d}\mu^{\mathrm{c}}_{\mathrm{w},T}}{\mathrm{d}x} - \frac{x_{\mathrm{N_2}}}{x_{\mathrm{O_2}}}\frac{\mathrm{d}\mu_{\mathrm{N_2},T}}{\mathrm{d}x} \quad (32)$$

we obtain

$$\sigma^{\mathrm{c}} = J'^{\mathrm{c}}_q\frac{\mathrm{d}}{\mathrm{d}x}\left(\frac{1}{T}\right) - j\frac{1}{T}\frac{\mathrm{d}\phi}{\mathrm{d}x} - J^{\mathrm{c}}_D\frac{1}{T}\frac{\mathrm{d}\mu^{\mathrm{c}}_{\mathrm{w},T}}{\mathrm{d}x} - \left(\frac{J_{\mathrm{N_2}}}{x_{\mathrm{N_2}}} - \frac{J_{\mathrm{O_2}}}{x_{\mathrm{O_2}}}\right)\frac{x_{\mathrm{N_2}}}{T}\frac{\mathrm{d}\mu_{\mathrm{N_2},T}}{\mathrm{d}x} \quad (33)$$

The interdiffusion flux of water and oxygen is

$$J^{\mathrm{c}}_D = \left(\frac{J^{\mathrm{c}}_{\mathrm{w}}}{x^{\mathrm{c}}_{\mathrm{w}}} - \frac{J_{\mathrm{O_2}}}{x_{\mathrm{O_2}}}\right)x^{\mathrm{c}}_{\mathrm{w}} = \left(\frac{J^{\mathrm{c}}_{\mathrm{w}}}{x^{\mathrm{c}}_{\mathrm{w}}} - \frac{j}{4Fx_{\mathrm{O_2}}}\right)x^{\mathrm{c}}_{\mathrm{w}} \quad (34)$$

so the transference coefficient corresponding to J^{c}_D is

$$t^{\mathrm{c}}_D = t^{\mathrm{c}}_{\mathrm{w}} - \frac{x^{\mathrm{c}}_{\mathrm{w}}}{4x_{\mathrm{O_2}}} \quad (35)$$

where $t^{\mathrm{c}}_{\mathrm{w}} = t^{\mathrm{m}}_{\mathrm{w}} + {}^1/_2$. The Peltier coefficient for the cathode side of the interface is

$$\pi^{\mathrm{c}} = T\left(\frac{1}{4}S_{\mathrm{O_2}} - S^{*,\mathrm{c}}_{\mathrm{e}} - t^{\mathrm{c}}_{\mathrm{w}}\,S^{\mathrm{c}}_{\mathrm{w}}\right) \quad (36)$$

The Peltier coefficient includes a contribution from water, as the water flux is contained in J'^{c}_q. As transported heat, we take $q^{*,\mathrm{c}} = -TS^{\mathrm{c}}_{\mathrm{w}}$. The Fourier-type thermal conductivity is λ^{c}, and the electric resistivity is r^{c}.

We now introduce the condition $J_{\mathrm{N_2}} = 0$ and the assumption that the chemical potential of water varies very little (we set the activity equal to unity). We next assume that the oxygen flux is not coupled to the other fluxes and that the flux is given

by the interdiffusion coefficient of oxygen in nitrogen, D^{c}_{ON}. This gives

$$\frac{dT}{dx} = -\frac{1}{\lambda^{c}}\left[J'^{c}_{q} - q^{*,c}_{w} J^{c}_{D} - \pi^{c}\frac{j}{F}\right]$$

$$\frac{d\phi}{dx} = -\frac{\pi^{c}}{TF}\frac{dT}{dx} - r^{c} j$$

$$\frac{dx_{O_2}}{dx} = \frac{j}{4FD_{ON}} \quad (37)$$

These equations and the energy balance are solved for the profiles of T, x_w, and ϕ in the cathode. The equations are solved with a mole fraction of oxygen at the right side boundary of $x^{0}_{O_2} = p_{O_2}/p^{0} = 0.21$.

3. Thermodynamic Data

Standard thermodynamic properties were taken from thermodynamic tables.[20] The hydrogen pressure was equal to the standard pressure $p^{0} = 1.013 \times 10^{5}$ Pa. The oxygen pressure was equal to that in air, $p_{O_2} = 0.21 \times p^{0}$, and the cell was operated at the anode temperature $T^{0} = 340$ K.

The expressions for the partial molar enthalpies and entropies were

$$H_i(T) = H_i^{0}(298\ \text{K}) + c_{p,i}(T - 298) \quad (38)$$

$$S_i(T) = S_i^{0}(298\ \text{K}) + c_{p,i}\ln\frac{T}{298} + R\ln x_i \quad (39)$$

At 298 K, the standard enthalpies of formation, $H_i^{0}(298\ \text{K})$, of liquid and vapor water are -285 and -242 kJ/mol, respectively. The heat capacities at constant pressure for hydrogen, oxygen, and liquid and vapor water are 29, 29, 75, and 34 J/(K mol), respectively. At 340 K, the standard enthalpies of hydrogen, oxygen, and liquid and water vapor became 1, 1, -284, and -242 kJ/mol. The standard entropies for hydrogen, oxygen, and liquid and vapor water at 298 K are 131, 205, 70, and 189 J/(K mol). The corresponding values at 340 K are 135, 210, 74, and 191 J/(K mol). The transported entropy of an electron in graphite was -2 J/(K mol).[21]

We assumed that all gases were ideal. The saturation pressure of water was found from tables and fitted to the temperature function

$$\log p^{*}_{w} = 5[-2.1794 + 0.02953(T - 273) - 9.1837 \times 10^{-5}(T - 273)^{2} + 1.4454 \times 10^{-7}(T - 273)^{3}] \quad (40)$$

The membrane density and molar mass were 1.64 kg/m^3 and 1.1 kg/mol, respectively. The thicknesses of the backing, surface, and membrane were 180, 10, and 127 μm, respectively.

A reference case was established with a set of transport data; see Table 1. For the anode surface resistivity and the porous graphite resistivities, we always took $r^{s} = 7.2 \times 10^{-6}$ ohm m^2 and $r^{a} = r^{c} = 10^{-4}$ ohm m^2, respectively.[6] For the thermal conductivity of the membrane, we always took the estimate of a water-filled polymer, $\lambda^{m} = 0.2$ W/(K m).[2] The values $\lambda^{a} = \lambda^{c} = 1$ W/(K m) were estimated from the thermal conductivity of porous graphite. The results were not sensitive to a 10-fold variation in these values.

The effective binary diffusion coefficients, D_{wH} and D_{ON}, in the reference case, were set to 2.5×10^{-6} m^2 s^{-1}. Vie[2] determined the thermal conductivity of the catalyst surfaces from experiments, $\lambda^{s,a} = \lambda^{s,c} = 1000$ W/(K m^2) from a model similar to this one but without coupling terms. We did not use the thermal conductivities on the membrane side of the surface in the calculation.

TABLE 1: Transport Data

transport property	dimension	reference case
$r^{a} = r^{c}$	ohm m	10^{-4}
$r^{s,a} = r^{s,c}$	ohm m^2	7.2×10^{-6}
λ^{m}	W/(K m)	0.2
$\lambda^{a} = \lambda^{c}$	W/(K m)	1
$\lambda^{s,a} = \lambda^{s,c}$	W/(K m^2)	10^{3}
$D_{wH} = D_{ON}$	m^2/s	5×10^{-5}
D_{m}	m^2/s	1.5×10^{-10}
j_0	A/m^2	2.5×10^{-3}
t^{m}_{w}		1.2
$q^{*,i}$	J/mol	$-T^{i}S^{i}$

The overpotential at the cathode in the same experiment was

$$\eta^{c} = \frac{2RT}{F}\ln\frac{j}{j_0} \quad (41)$$

with the exchange current density for oxygen in air of $j_0 = 2.5 \times 10^{-3}$ A/m^2.[2] The membrane diffusion coefficient $D^{m} = 6 \times 10^{-11}$ m^2 s was taken from Springer et al.[18] (The number refers to the membrane water content $\lambda = 14$ mol water/mol ionic sites.)

The transference coefficient of water in Nafion 115 in equilibrium with vapor was 1.2.[22] The Peltier coefficients for the anode and cathode were calculated from eqs 14 and 36. The Peltier heat for the membrane was taken from measurements $\pi^{m}/T^{m} = 13$ J/(K mol).[23] The heats of transfer in the various parts of the system were chosen in agreement with eq 50. By the choice of the first $q^{*,m}$ of pure water, the subsequent values for the membrane and the cathode backing were found.

4. Calculations

The energy balances and the sets of flux equations were solved by iterations, for a low (500 A/m^2), a medium (2500 A/m^2), and a high (5000 A/m^2) current density. The water and heat fluxes in the anode backing were initially estimated and adjusted after integrating through the layers, until the temperature at the cathode outlet, $T^{c,0}$, was 340 K, and the given equilibrium conditions for water were fulfilled. For lack of information of transport data, we did not use eqs 22c and 29a in the solution procedure but set the membrane temperature equal to the surface temperature on both sides.

The set of equations for each subsystem was solved using Matlab 6.0.088 from MathWorks on an ordinary PC. The current densities gave physical solutions to the equations with positive mole fractions at and in the membrane. The boundary temperature of the anode and cathode layers were always $T^{0,a} = T^{0,c} = 340$ K.

For 2500 A/m^2, we studied the sensitivity of the solution to transport coefficients in the following cases:

1. All coupling coefficients, except the electro-osmotic coefficient in the membrane, were set to zero. This way of solving equations is now common in the literature.[1]

2. The cathode overpotential was set to zero, by setting the exchange current density equal to the current density.

3. The thermal conductivities of the surfaces were varied. There is little knowledge in the literature about these properties

4. The interdifusion coefficients of the gases were varied to find the effect of a limiting supply of gas. The water diffusion coefficient was varied to see if back-diffusion of water was significant.

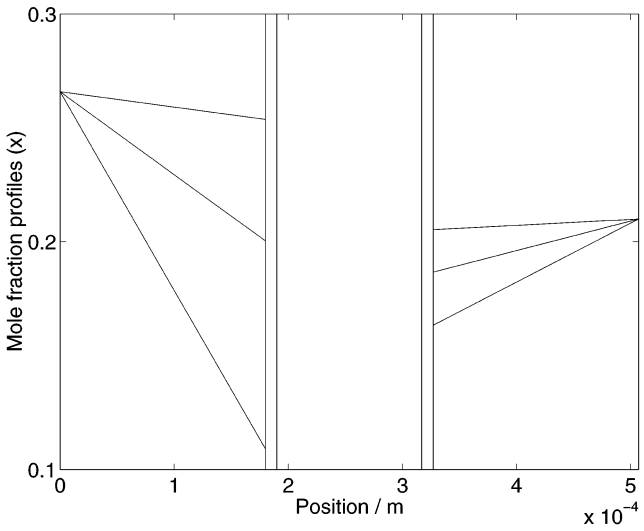

Figure 2. Mole fraction profile of water (left) and oxygen (right) as a function of current densities 500, 2500, and 5000 A/m^2. The lower curves arise with the highest current densities.

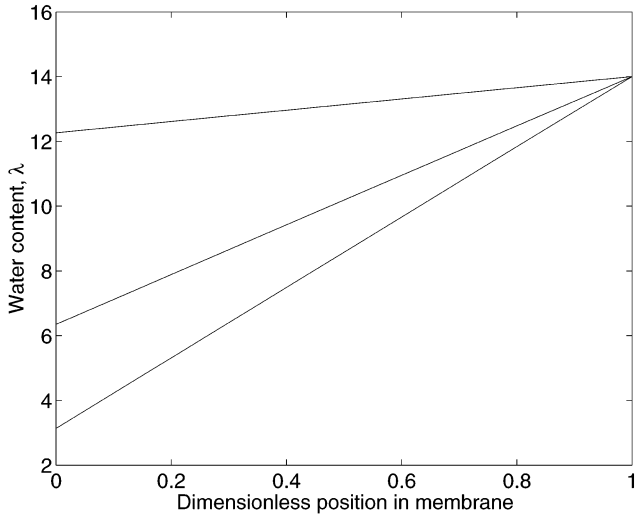

Figure 3. Water content in moles per ionic site across the membrane as a function of current densities 500, 2500, and 5000 A/m^2. The lower curves rise with the highest current densities.

5. The membrane resitivity was varied

The local entropy production was calculated after the profiles in temperature, composition, and electric potential were obtained. The integrated values from eq 6 were in the end compared to the results from the overall balance, eq 5.

5. Results

The mole fraction profiles for water and oxygen in the diffusion backing, the water-content profile in the membrane, the electric potential profile, and the temperature profile are shown for three current densities in a reference case in Figures 2−5. The corresponding heat fluxes and the accumulated entropy production across the cell are shown in Figures 6 and 7.

The mole fractions of water and of oxygen varied essentially linearly across the anode and cathode diffusion backing; see Figure 2. We found a linear variation also across the membrane in the membrane water content; see Figure 3. For the current density 2500 A/m^2, the water flux into the anode was 0.0175 mol/(m^2 s), while it was 0.0304 mol/(m^2 s) out of the cathode.

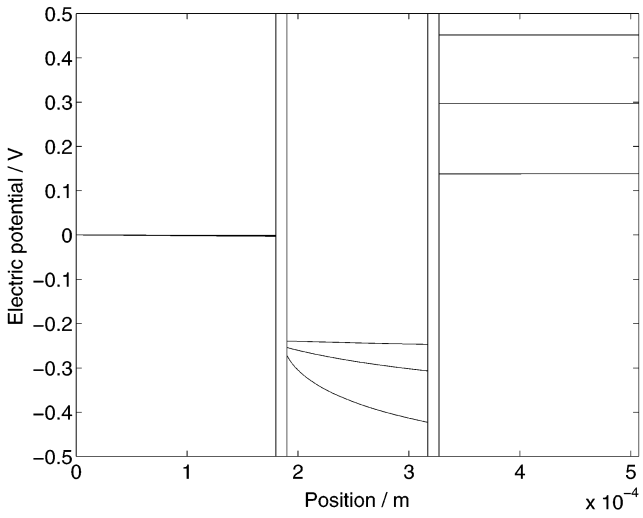

Figure 4. Electric potential profile across the cell as a function of current densities 500 (upper curves), 2500 (middle curves), and 5000 A/m^2 (lower curves).

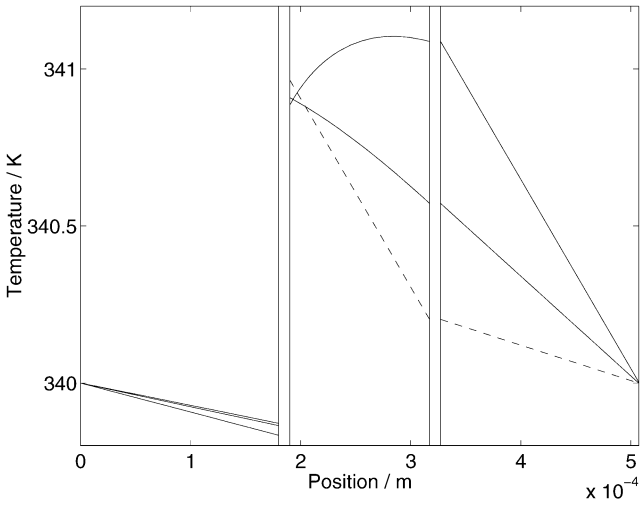

Figure 5. Temperature profile across the cell as a function of current densities 500 (broken line), 2500 (lower unbroken lines), and 5000 (upper unbroken lines) A/m^2.

The electric potential profile varied also linearly in the backings. At the electrode surfaces, it jumped due to the electrode reactions; see Figure 4. In the membrane, the profile was significantly curved at high current densities due to the water-content-dependent resistivity of the membrane. The curvature is larger close to the anode, where the water content is small; cf. Figure 2. The potential drop at the anode is large, mainly due to the entropy of hydrogen. At the lowest current density, the potential rose to nearly 0.5 V at the cathode. The value is low because the cell produces liquid water from oxygen in air.

The temperature profiles were also linear in the bulk phases, had (small) jumps at the surfaces, and varied in the membrane in a nonlinear way for high current densities; see Figure 5. The temperature of the cathode surface was smaller than that of the anode for small current densities, but this changed to the reverse situation as the current density increased. The effect of the Peltier heat sink at the anode can be seen in the figure. It gives a negative slope of the temperature profile on the left-hand side of the membrane.

The entropy production rate in each subsection was found by integrating across each subsystem. The accumulated entropy

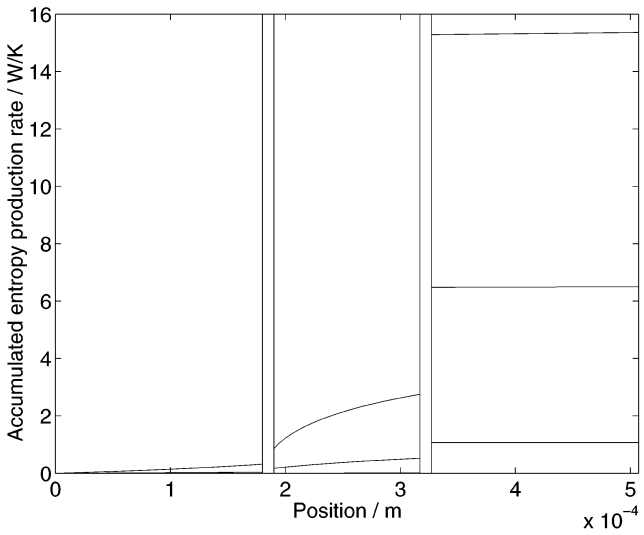

Figure 6. Accumulated entropy production rate for current densities of 500, 2500, and 5000 A/m^2. The upper curve is due to the highest current density.

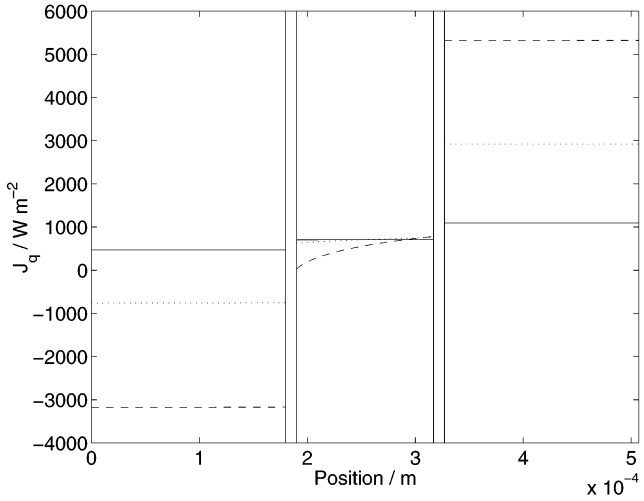

Figure 7. Heat fluxes in the cell as a function of current densities 500 (unbroken line), 2500 (dotted curve), and 5000 (dashed curve) A/m^2.

production rate is shown in Figure 6. It varies largely with the current density, as expected. Most of the entropy is always produced at the cathode, but the entropy production in the membrane is also significant. The accumulated entropy production rate was always equal to the entropy flux out of the cell minus the entropy flux into the cell, as it should be according to eqs 5 and 6.

The corresponding values of the heat fluxes are shown in Figure 7. A positive value in the cathode section means that the flux is directed out of the cathode. The negative value obtained in the anode section means that the flux is directed out of the anode. Most striking is that the heat fluxes out of the system have very different magnitudes. It is not so that heat is escaping the single fuel cell in a symmetrical manner. The heat flux in the membrane is positive for small current densities and negative for for high current densities.

In case 1, we found that removal of all thermal coupling terms had no effect the entropy production, but a relatively large impact on the heat fluxes was found. The negative slope seen in the temperature profile of the anode disappeared (evidence for it being due to the Peltier effect), and the heat fluxes in Figure 7 changed in absolute value by 10−20%.

In case 2, we found that a reduction in the overpotential in the cathode surface had a substantial effect on $\sigma^{s,c}$ (from 6.5 to 0.6 J/(m^2 s)). The magnitude of the heat fluxes changed accordingly. At the cathode, the heat flux dropped from 2800 to 1400 W/m^2. It did not have any significant effect on the entropy production in other parts of the cell.

In case 3, we observed that the thermal conductivities of the backing and the electrode surface were important for the heat fluxes and the shape of the temperature profiles. A reduction in the thermal conductivity of the porous graphite by a factor of 2 lowered the heat flux in the anode to −1200 W/m^2 and in the cathode to 2500 W/m^2. The entropy production rate changed at most 1% in these cases.

In case 4, we found that the diffusion coefficient for water in the membrane has a small effect on the entropy production rate, but its value is very important for the possibility to find a solution to the problem. It was not possible to find a solution by reducing its value more than 50%. By the diffusion coefficient changing this much, the heat flux in the anode changed to −1000 W/m^2 for the given current density.

The value of the gas diffusion coefficient was important for access of water to the anode side for the current densities used here. This can be seen from the lower curve to the left in Figure 2. No limitations were found for the oxygen or hydrogen fluxes, with the conditions used here. Also, the mass fluxes in the backing were furthermore not important for the dissipation of energy. This can be seen from Figure 6; the curve is flat in these regions.

The varying membrane resitivity given by Springer et al.[18] gave a significant contribution to the entropy production. The value for a membrane saturated with water, like the value used by Nguyen et al.,[24] did not give such an effect.

6. Discussion

The main purpose of this work was to describe a method that can be used to calculate the local and total entropy production in an electrochemical cell and show how to obtain a simultaneous set of profiles for concentration, electric potential, and temperature. The theoretical section of the paper gave a systematic procedure for such a calculation. A model, consistent with the second law of thermodynamics, was constructed for the coupled transport of heat, mass, and charge that take place in five consecutive layers in a heterogeneous one-dimensional fuel cell. Nonequilibrium thermodynamics for the two surfaces define proper boundary conditions for the three bulk phases. The problem posed by the finite thickness of the surface layer[8] can be solved in this manner. This theoretical method was used previously[6,16] but not to the extent that is done here. The present system is complicated, but we hope to have contributed to a general procedure for a physical-chemical description of batteries, fuel cells, and electrolysis cells.

A solution to the transport problem was found for a set of data and assumptions called the reference case, at a small, medium, and large current density. The lack of knowledge of surface transport properties made it necessary to introduce several assumptions, most importantly the assumption of equilibrium for water at each surface. This posed a strong restriction on the solution space; a physical solution was only obtained within a limited range of diffusion coefficients of the system. The solutions confirm much of the state of the art knowledge about the system, but new details are added. The values of the heat fluxes, the accumulated entropy production, and the electric potential and the temperature profiles are new or improved upon

earlier work.[6,7] We therefore discuss these issues before we give a perspective on the total solution.

6.1. Water and Oxygen Profiles and Transports. The linear profiles (Figure 2) for the mole fractions of water in the anode backing and for oxygen in the cathode backing are well-known and were expected.

The model was constructed so that the mole fraction of water decreased toward the membrane, because the water transference number (moles of water transported per proton) was larger than unity ($t_w^m = 1.2$). With a constant pressure, it follows that hydrogen accumulates in front of the surface. There is then no limitation on the electrode reaction from hydrogen. A deficiency in water can arise at constant pressure at high current densities, as seen by the lower curve to the left in Figures 1 and 2. The water-content profile in the membrane was similar to the one presented earlier.[6] The hydrogen in front of the surface determines the large drop in electric potential at the anode surface in Figure 4; see below for a further discussion.

At the highest current density, the reduction in the oxygen mole fraction at the cathode surface is 25% of the level in air. This reduction is not critical (rate-limiting) for the cathode reaction.

The asymmetry in the water transport into and out of the cell is well-known.[5] Asymmetry is expected because water is produced on the cathode side. For the intermediate current density, the supply of water to the anode is about half the flux out of the cathode. The water supply into the anode is thus almost solely given by the term $t_w^m j/F$, compatible with little diffusion of water across the membrane from the cathode to the anode. The term $t_w^m j/F$ is crucial for the membrane state on the anode side, in agreement with earlier findings.[5]

These results must be seen with the background that the model assumes a fixed porosity and no clogging of the pores by water. Many authors have found that such factors are important for access of O_2; see, for example, refs 5 and 24. They should be included in further studies along these lines.

The entropy production due to the interdiffusion of hydrogen and water and oxygen and nitrogen is negligible; see Figure 6 and the discussion below. This is not according to conventional wisdom for the current densities used here; see, for example, ref 8. Because our model is tested for consistency not only with the first but also with the second law, we trust our results.

6.2. Electric Potential Profiles. The electric potential profiles have some parts that are familiar and some parts that are less familiar. There is practically no variation in the anode or cathode backing; see Figure 4. This is expected for such small resistances and gradients. A potential drop in the anode surface has not been presented before but can explained simply by the disappearance of hydrogen. The entropy of hydrogen is a large quantity and therefore a large part of its chemical potential. It is common to take a zero potential drop at this electrode, but this is thus not correct.

The largest increment in the electric potential occurs at the cathode surface, of course. This is the important location for conversion of the reaction Gibbs energy into electric energy. We see that the jump is reduced as the current density increases, in a nonlinear way, as predicted from the variation in the overpotential.

The nonlinear electric potential profile in the membrane at high current densities can be explained by the strong water-content dependence of the membrane resistivity. We find that the processes in the membrane reduce the positive electric potential of the cell more than a reduction in the mole fraction of oxygen in the cathode diffusion backing. The nonlinear variation in this contribution is thus an alternative or supplementary explanation for the nonlinear drop in the polarization curve at relatively high current densities.[8] The variation in the entropy production across the cell supports this interpretation; see section 6.4 below.

The difference in potential between the cell boundaries gives the cell potential. When plotted as a function of the current density, we obtain the polarization curve (not shown).

6.3. Heat Fluxes and Temperature Profiles. Knowledge about the heat fluxes is important for design of the heat exchange system of the cell. The importance of this was already pointed out by Fuller and Newman.[9] From knowledge about the natural paths of escape, one can enhance or counteract the heat fluxes by introducing sinks/sources, regulate gas velocities, etc. In Figure 7, we see that heat is coming out of the sides of the cell in an asymmetric way. The heat fluxes out of the cell differ by approximately a factor of 2. The asymmetry is highly sensitive to thermal conductivities and boundary temperatures,[7] however, and these are essentially unknown in practice. It should also be remembered that we are here calculating a one-dimensional case. The heat fluxes should depend on the actual geometry.

Even if the thermal coupling coefficients do not have any impact on the entropy production (Results, case 1), they are important for giving the correct value of the heat fluxes and required to have a thermodynamically consistent model. To see this, take as an example the expression for the heat flux in the anode

$$J_q'^{a} = -\lambda^{a}\frac{dT}{dx} + q^{*,a}J_w^a + \pi^a\frac{j}{F} \qquad (42)$$

We found that all three contributions to $J_q'^{a}$ were significant. Figure 5 demonstrates that the two last terms are in fact larger than the first, since $J_q'^{a} < 0$ and $dT/dx > 0$. Similar observations have been reported for evaporation and condensation.[25]

The largest change in the temperature profile with current density occurred around the cathode, and this reflects the dissipation by the cathode overpotential. This is expected. This temperature is also most sensitive to the thermal conductivities of the surfaces and the backing.

But with current densities below 5000 A/m^2, we found that the cell is isothermal for all practical measures; see Figure 5. The temperature rise inside the cell was negligible with the boundary conditions and transport data used. This may seem contrary to recent experiments.[2,3] One must then remember the impact of the boundary conditions. They were different in the experiments reported and here. In the experiments, there were no thermostats to remove all heat from the cell; on the contrary, the cell house was normally heated to an elevated temperature. In the calculations, we demanded that the temperature is 340 K on both sides. The set of boundary conditions we used earlier[7] gave large temperature jumps because $T^{c,0}$ was set free.

6.4. Entropy Production Rates. The accumulated entropy production rate across the cell was given in Figure 6. We conclude from these numbers and the calculated cases 1−5 that the entropy production is always negligible in the backing of the anode and of the cathode. The entropy production is largest in the cathode surface and next largest in the membrane and anode surface. The relative importance of the membrane as a dissipator grows when the current density increases, and the anode side becomes relatively dry. The nonlinear increase in the membrane resistivity with water content explains why the loss in the membrane grows nonlinearly.

The shape of the polarization curve can also be used to discuss energy losses in the cell. This curve ranks the overpotential as

the most important cause of dissipation, before the ohmic resistivities. The same is obtained from the entropy production rate. The nonlinear part of the polarization curve for high current densities has been explained by diffusional losses. It is clear that the chemical potential of the reactants at the catalysts determines the value of the electric potential. But in this case, that was of minor importance. We see from Figure 6 that this part of the curve also can be explained by the increased membrane resistivity.

The accumulated entropy production agreed with the result from the total entropy balance within the numerical accuracy of the calculations. It is comforting to know that five local models with input of various transport data in the end give the same result as calculated directly from the partial molar entropies, the molar fluxes, and the heat fluxes.

In Appendix A, we showed that neglect of thermal coupling coefficients in the model leaves the total entropy production rate of the cell unaltered. (An incorrect statement was made about this earlier, at a time when we had not yet obtained a consistent model.[7]) The present calculations confirmed this invariance. The heats of transfer or entropies of transfer obey certain overall transformation properties for the entropy change and the enthalpy change of the total system.[12,25] They are nonzero and significant at the interfaces and largely unknown for many systems. They have partially been estimated in the present work.

7. Conclusions

We have demonstrated how nonequilibrium thermodynamics can be used to characterize the energy conversion in heterogeneous electrochemical cells. We have presented a simultaneous set of solutions for concentration, electric potential, and temperature profiles across a single polymer electrolyte fuel cell using literature data for a Nafion 115 membrane and a limiting assumption about equilibrium for water across the surfaces. We have also calculated the local entropy production in each subsystem of the cell. The local values were integrated across the cell and agreed then with the total entropy balance for the cell.

The solutions were found under constraints that may not be realistic and limit the possibility to find solutions. For instance, the condition of equilibrium of water at each interface limits the possible flux of water and possible surface temperatures. This is because the vapor pressure at equilibrium is a unique function of the temperature. The main point was not to give concrete facts, however, but to demonstrate a physical-chemical method of calculation that can give the type of information presented here.

We have also shown that measurements are needed to improve on the calculations. For instance, we have only estimated a value for $q^{*,a}$ and have a rather limited knowledge of the surface thermal conductivities. These quantities should be measured.

The largest reduction in entropy production or increase in power output can here be obtained by reducing the overpotential of the cathode. This is well-known. Less well-known is the relatively large dissipation in the membrane. It is larger than the energy dissipated in the electrode backings.

We have found that heat most likely escapes the cell in an asymmetric manner, largely dependent on the thermal conductivity of the backing and of the surfaces, the water diffusion coefficient, the resistivity of the membrane, and the state of water at the surfaces. It will be interesting to see if the asymmetry will continue to be there when the cell model is improved. Knowledge of lost work and local heat production may be important for auxiliary equipment design and for further research planning for fuel cells and batteries.[11]

Acknowledgment. A. R. thanks Statoil Vista for grant support of this work.

Symbol List

a_w = water activity
c_w= water concentration, mol/m^3
D_{ij} = interdiffusion coefficient of i and j, m^2/s
F = Faraday's constant, 96 500 C/mol
ϕ = electric potential, V
$\Delta_r G$ = reaction Gibbs energy, J/mol
H_i = partial molar enthalpy, J/mol
$\Delta_{vap}H$ = enthalpy of evaporation, J/mol
η^c = cathode overpotential, V
j = electric current density, A/m^2
J'_q = flux of heat, J/(s m^2)
J_i = flux of component, mol/(s m^2)
l_{ij}, L_{ij} = phenomenological coefficients
λ = water content, mol/mol ionic site
λ^i = thermal conductivity of i, W/(m K)
λ^s = thermal conductivity of surface, W/(m^2 K)
M = molar mass of Nafion polymer, kg/mol
μ_i = chemical potential of i, J/mol
p_i = pressure, Pa
π = Peltier coefficient, J/mol
q^* = heat of transfer, J/mol
R = gas constant, 8.314 J/(K mol)
r^i = resistivity of i, ohm m
r^s = resistivity of surface, ohm m^2
ρ = membrane dry density, kg/m^3
S_i = entropy, J/(K mol)
S_i^* = transported entropy, J/(K mol)
σ = entropy production rate, J/(K m^3)
σ^s = entropy production rate of surface, J/(K m^2)
T = temperature, K
t_w = transference coefficient
x_i = mole fraction
x = coordinate axis, m

Appendix A: Entropy Balance

The entropy production can be calculated from the entropy balance for the complete system. The entropy balance at stationary state over a system gives the entropy production (per unit area) in the system from

$$\frac{dS_{irr}}{dt} = J_S^{c,0} - J_S^{a,0} \tag{43}$$

where c and a stands for cathode and anode, respectively, and 0 gives the boundary position at the channel. The entropy flux is defined by[12]

$$J_S = \frac{J'_q}{T} + \Sigma_i J_i S_i \tag{44}$$

Here, J'_q is the measurable heat flux, J_i is the mass flux of component i, S_i is the partial molar entropy of i, and T is the temperature. The summation is carried out over all independent components. In the single, one-dimensional fuel cell, the component fluxes are of oxygen, hydrogen, and water. The

component fluxes carry entropy, giving from eqs 44 and 43

$$\frac{\mathrm{d}S_{\mathrm{irr}}}{\mathrm{d}t}=\left(\frac{J'^{\mathrm{c},0}_q}{T^{\mathrm{c},0}}+J^{\mathrm{c}}_{\mathrm{w}}S^{\mathrm{c},0}_{\mathrm{w}}+J_{\mathrm{O}_2}S^{\mathrm{c},0}_{\mathrm{O}_2}\right)-\left(\frac{J'^{\mathrm{a},0}_q}{T^{\mathrm{a},0}}+J^{\mathrm{a}}_{\mathrm{w}}S^{\mathrm{a},0}_{\mathrm{w}}+J_{\mathrm{H}_2}S^{\mathrm{a},0}_{\mathrm{H}_2}\right) \tag{45}$$

The relations between the mass fluxes given in section 2.1 can now be introduced, and we obtain

$$\frac{\mathrm{d}S_{\mathrm{irr}}}{\mathrm{d}t}=\frac{J'^{\mathrm{c},0}_q}{T^{\mathrm{c},0}}-\frac{J'^{\mathrm{a},0}_q}{T^{\mathrm{a},0}}+\frac{j}{F}\left[\frac{1}{2}(S^{\mathrm{c},0}_{\mathrm{w}}-S^{\mathrm{a},0}_{\mathrm{H}_2})-\frac{1}{4}S^{\mathrm{c},0}_{\mathrm{O}_2}\right]+J^{\mathrm{a}}_{\mathrm{w}}(S^{\mathrm{c},0}_{\mathrm{w}}-S^{\mathrm{a},0}_{\mathrm{w}}) \tag{46}$$

To see the role of the coupling terms in the heat fluxes, consider the simpler case, when there is no nitrogen present. The heat fluxes in the backings are then both as given in Appendix B below or subsection 2.2. We introduce these and obtain

$$\frac{\mathrm{d}S_{\mathrm{irr}}}{\mathrm{d}t}=-\frac{\lambda^{\mathrm{c}}}{T^{\mathrm{c},0}}\left(\frac{\mathrm{d}T}{\mathrm{d}x}\right)^{\mathrm{c}}+\frac{q^{*,\mathrm{c}}}{T^{\mathrm{c},0}}\left(J^{\mathrm{c}}_D-t^{\mathrm{c}}_D\frac{j}{F}\right)+\frac{\pi^{\mathrm{c}}}{T^{\mathrm{c},0}}\frac{j}{F}+\frac{\lambda^{\mathrm{a}}}{T^{\mathrm{a},0}}\left(\frac{\mathrm{d}T}{\mathrm{d}x}\right)^{\mathrm{a}}-\frac{q^{*,\mathrm{a}}}{T^{\mathrm{a},0}}\left(J^{\mathrm{a}}_D-t^{\mathrm{a}}_D\frac{j}{F}\right)-\frac{\pi^{\mathrm{a}}}{T^{\mathrm{a},0}}\frac{j}{F}+\frac{j}{F}\left[\frac{1}{2}(S^{\mathrm{c},0}_{\mathrm{w}}-S^{\mathrm{a},0}_{\mathrm{H}_2})-\frac{1}{4}S^{\mathrm{c},0}_{\mathrm{O}_2}\right]+J^{\mathrm{a}}_{\mathrm{w}}(S^{\mathrm{c},0}_{\mathrm{w}}-S^{\mathrm{a},0}_{\mathrm{w}}) \tag{47}$$

The next step is to introduce the expressions for the Peltier coefficients, eqs 14 and 36

$$\frac{\pi^{\mathrm{c}}}{T^{\mathrm{c},0}}=\frac{1}{4}S^{\mathrm{c},0}_{\mathrm{O}_2}-S^{*,\mathrm{c},0}_{\mathrm{e}}-\frac{1}{2}S^{\mathrm{c},0}_{\mathrm{w}} \tag{48}$$

$$\frac{\pi^{\mathrm{a}}}{T^{\mathrm{a},0}}=-\frac{1}{2}S^{\mathrm{a},0}_{\mathrm{H}_2}-S^{*,\mathrm{a},0}_{\mathrm{e}} \tag{49}$$

The difference in the Peltier coefficients cancel with the entropy of the reaction, when $S^{*,\mathrm{a},0}_{\mathrm{e}}=S^{*,\mathrm{c},0}_{\mathrm{e}}$. This is so because the heat effect connected with conversion of reactants to products does not contribute to the entropy production but to the electric work.

For both electrode backings, we find the combination $J^{\mathrm{i}}_D-t^{\mathrm{i}}_D j/F=J^{\mathrm{i}}_{\mathrm{w}}$ where i = a, c (Appendix B). The terms containing the heats of transfer disappear in the overall expression. The terms containing the heats of transfer must then be opposite and equal to the term that contains the water flux. These terms are reversible in nature and do not give any net entropy production. As a consequence

$$\frac{q^{*,\mathrm{c}}}{T^{\mathrm{c},0}}-\frac{q^{*,\mathrm{a}}}{T^{\mathrm{a},0}}=-S^{\mathrm{c},0}_{\mathrm{w}}+S^{\mathrm{a},0}_{\mathrm{w}} \tag{50}$$

An estimate for $q^{*,\mathrm{a}}$ is therefore $-TS^{\mathrm{a}}_{\mathrm{w}}$. The (net) entropy production in the cell ends up as heat conducted from the surroundings, as it should. There is a large difference between using the full expression or only a part of the expression for the J'_q values, however. With these relations, we also obtain

$$\frac{\mathrm{d}S_{\mathrm{irr}}}{\mathrm{d}t}=-\frac{\lambda^{\mathrm{c}}}{T^{\mathrm{c},0}}\left(\frac{\mathrm{d}T}{\mathrm{d}x}\right)^{\mathrm{c}}+\frac{\lambda^{\mathrm{a}}}{T^{\mathrm{a},0}}\left(\frac{\mathrm{d}T}{\mathrm{d}x}\right)^{\mathrm{a}} \tag{51}$$

Numerical solutions of the local transport problems are in agreement with the second law, if these expressions for the entropy production rate all apply. In the present study, this was verified.

Appendix B: Flux Equations for the Backings

We show how the entropy production rate gives the flux equations to be solved. The same derivation can be used for the anode and the cathode. In section 2.2, we found the entropy production rate

$$\sigma=J'_q\frac{\mathrm{d}}{\mathrm{d}x}\left(\frac{1}{T}\right)-j\frac{1}{T}\frac{\mathrm{d}\phi}{\mathrm{d}x}-J_D\frac{1}{T}\frac{\mathrm{d}\mu_{\mathrm{w},T}}{\mathrm{d}x} \tag{52}$$

The interdiffusion flux J_{D} is for hydrogen, water, and the anode and for oxygen and water in the cathode. The linear flux−force relations that follow from eq 52 are, according to Onsager[12]

$$J'_q=L_{qq}\frac{\mathrm{d}}{\mathrm{d}x}\left(\frac{1}{T}\right)-L_{q\mu}\frac{1}{T}\frac{\mathrm{d}\mu_{\mathrm{w},T}}{\mathrm{d}x}-L_{q\phi}\frac{1}{T}\frac{\mathrm{d}\phi}{\mathrm{d}x} \tag{53}$$

$$J_D=L_{\mu q}\frac{\mathrm{d}}{\mathrm{d}x}\left(\frac{1}{T}\right)-L_{\mu\mu}\frac{1}{T}\frac{\mathrm{d}\mu_{\mathrm{w},T}}{\mathrm{d}x}-L_{\mu\phi}\frac{1}{T}\frac{\mathrm{d}\phi}{\mathrm{d}x} \tag{54}$$

$$j=L_{\phi q}\frac{\mathrm{d}}{\mathrm{d}x}\left(\frac{1}{T}\right)-L_{\phi\mu}\frac{1}{T}\frac{\mathrm{d}\mu_{\mathrm{w},T}}{\mathrm{d}x}-L_{\phi\phi}\frac{1}{T}\frac{\mathrm{d}\phi}{\mathrm{d}x} \tag{55}$$

where L_{ij} are phenomenological coefficients. Superscripts that show the subsystem have been omitted for the time being. There are only six independent coefficients, because we have three relations of the type $L_{\mathrm{ij}}=L_{\mathrm{ji}}$ (Onsager relations). Before we define the coefficients, we rewrite the set of equations. We first eliminate the electric potential gradient in the heat and mass fluxes. This gives

$$J'_q=l_{qq}\frac{\mathrm{d}}{\mathrm{d}x}\left(\frac{1}{T}\right)-l_{q\mu}\frac{1}{T}\frac{\mathrm{d}\mu_{\mathrm{w},T}}{\mathrm{d}x}+\frac{L_{q\phi}}{L_{\phi\phi}}j \tag{56}$$

$$J_D=l_{\mu q}\frac{\mathrm{d}}{\mathrm{d}x}\left(\frac{1}{T}\right)-l_{\mu\mu}\frac{1}{T}\frac{\mathrm{d}\mu_{\mathrm{w},T}}{\mathrm{d}x}+\frac{L_{\mu\phi}}{L_{\phi\phi}}j \tag{57}$$

$$j=L_{\phi q}\frac{\mathrm{d}}{\mathrm{d}x}\left(\frac{1}{T}\right)-L_{\phi\mu}\frac{1}{T}\frac{\mathrm{d}\mu_{\mathrm{w},T}}{\mathrm{d}x}-L_{\phi\phi}\frac{1}{T}\frac{\mathrm{d}\phi}{\mathrm{d}x} \tag{58}$$

where the coefficients are related by

$$l_{\mathrm{ij}}=L_{\mathrm{ij}}-\frac{L_{\phi\mathrm{i}}L_{\mathrm{j}\phi}}{L_{\phi\phi}} \tag{59}$$

We now define the transference coefficient

$$t_D=\left(\frac{J_D}{j/F}\right)_{\mathrm{d}\mu_{\mathrm{w}}=0,\mathrm{d}T=0}=F\frac{L_{\mu\phi}}{L_{\phi\phi}} \tag{60}$$

the Peltier coefficient

$$\pi=\left(\frac{J'_q}{j/F}\right)_{\mathrm{d}\mu_{\mathrm{w}}=0,\mathrm{d}T=0}=F\frac{L_{q\phi}}{L_{\phi\phi}} \tag{61}$$

and the heat of transfer

$$q^*=\left(\frac{J'_q}{J_D}\right)_{j=0,\mathrm{d}T=0}=\frac{l_{q\mu}}{l_{\mu\mu}} \tag{62}$$

The transference coefficient gives the interdiffusion flux connected with charge transfer for zero chemical potentials and constant temperature. The Peltier coefficient is the (measurable) heat transport that accompanies the charge transport. The heat of transfer is the heat transported for the given mass flux at $j=0$, in an isothermal system.

We introduce these definitions into the last set of flux equations, solve the expression for J_{D} for the gradient in the

mole fraction of water, and introduce the expression for dx_w/dx into the heat flux. The result is

$$J'_q = -\left(\frac{l_{qq}}{T^2} - \frac{(q^*)^2 l_{\mu\mu}}{T^2}\right)\frac{dT}{dx} + q^*\left(J_D - t_D\frac{j}{F}\right) + \pi\frac{j}{F} \quad (63)$$

$$J_D = -\frac{q^* l_{\mu\mu}}{T^2}\frac{dT}{dx} - l_{\mu\mu}\frac{1}{T}\frac{d\mu_{w,T}}{dx} + t_D\frac{j}{F} \quad (64)$$

$$\frac{d\phi}{dx} = -\frac{\pi}{TF}\frac{dT}{dx} - \frac{t_D}{F}\frac{d\mu_{w,T}}{dx} - \frac{jT}{L_{\phi\phi}} \quad (65)$$

We can now introduce as main transport coefficients the interdiffusion coefficient of water and gas (hydrogen or oxygen) in an ideal gas mixture

$$D_{wg} = l_{\mu\mu}R/x_w \quad (66)$$

the specific electric resistivity

$$r = T/L_{\phi\phi} \quad (67)$$

and the stationary state thermal conductivity

$$\lambda = \frac{l_{qq}}{T^2} - \frac{(q^*)^2 D_{wg} x_w}{RT^2} \quad (68)$$

The three main coefficients and the three coupling coefficients characterize the transport of heat, mass, and charge through each layer. They are well-defined through experiments. The magnitude of the coefficients may vary from layer to layer. The coefficients can be introduced into the flux equations, and these can now be solved for the gradients in temperature, concentration, and electric potential. We obtain the expressions that were used in subsection 2.2

$$\frac{dT}{dx} = -\frac{J'_q}{\lambda} + \frac{q^*}{\lambda}\left(J_D - t_D\frac{j}{F}\right) + \pi\frac{j}{F\lambda} \quad (69)$$

$$\frac{dx_w}{dx} = -\frac{q^* x_w}{RT^2}\frac{dT}{dx} - \frac{\left(J_D - t_D\frac{j}{F}\right)}{D_{wg}} \quad (70)$$

$$\frac{d\phi}{dx} = -\frac{\pi}{TF}\frac{dT}{dx} - \frac{t_D RT}{Fx_w}\frac{dx_w}{dx} - rj \quad (71)$$

In the anode gas channel (subsection 2.2), the chemical potential of water vapor at constant temperature was described by

$$\frac{1}{T}\frac{d\mu_{w,T}}{dx} = \frac{R}{x_w}\frac{dx_w}{dx} \quad (72)$$

In the cathode gas channel (subsection 2.6), the expressions were further simplified by setting the water chemical potential constant (unit activity for water).

Appendix C: Flux Equations for the Membrane

For the membrane, we would like to introduce the water content (in moles per ionic site in the membrane) as a variable in the transport equations. The water content is

$$\lambda = c_w M/\rho \quad (73)$$

Here, M is the molar mass of the polymer in the membrane, and ρ is the membrane dry density.

We start with the entropy production rate for transport of heat, water, and charge (protons)

$$\sigma^m = J'^m_q \frac{d}{dx}\left(\frac{1}{T}\right) - J^m_w \frac{1}{T}\frac{d\mu^m_{w,T}}{dx} - j\frac{1}{T}\frac{d\phi^m}{dx} \quad (74)$$

The procedure that gave eqs 63 is used again, now for the membrane

$$J'^m_q = -\left(\frac{l^m_{qq}}{T^2} - \frac{(q^{*,m})^2 l_{\mu\mu}}{T^2}\right)\frac{dT}{dx} + q^{*,m}\left(J^m_w - t^m_w\frac{j}{F}\right) + \pi^m\frac{j}{F} \quad (75)$$

$$J^m_w = -\frac{q^{*,m} l^m_{\mu\mu}}{T^2}\frac{dT}{dx} - l^m_{\mu\mu}\frac{1}{T}\frac{d\mu^m_{w,T}}{dx} + t^m_w\frac{j}{F} \quad (76)$$

$$\frac{d\phi^m}{dx} = -\frac{\pi^m}{TF}\frac{dT}{dx} - t^m_w\frac{1}{F}\frac{d\mu^m_{w,T}}{dx} - r^m j \quad (77)$$

The stationary state thermal conductivity and the electric resistivity are defined as before

$$\lambda^m = \left(\frac{l^m_{qq}}{T^2} - \frac{(q^{*,m})^2 l^m_{\mu\mu}}{T^2}\right) \quad (78)$$

$$r^m = L^m_{\phi\phi}/T \quad (79)$$

The water transference number is

$$t^m_w = \left(\frac{J^m_w}{j/F}\right)_{d\mu_{w,T}=0,dT=0} \quad (80)$$

The diffusion coefficient of water in the membrane is defined through

$$l^m_{\mu\mu} = D^m_w\frac{c_w}{R} \quad (81)$$

The water in the membrane is not ideal, so we would like to take advantage of the (experimental) relation between the water activity and the water content[18]

$$\lambda(a_w < 1) = 0.043 + 17.81a_w - 39.85a_w{}^2 + 36.0a_w{}^3$$
$$\lambda(1 < a_w < 3) = 14 + 1.4a_w$$
$$\lambda(a_w > 3) = 16.8 \quad (82)$$

The mass flux becomes

$$J^m_w = -\frac{q^{*,m} D^m_w \lambda\rho}{RMT^2}\frac{dT}{dx} - \frac{D^m_w\rho}{M}\frac{d\lambda_w}{dx} + t^m_w\frac{j}{F} \quad (83)$$

The water activity at the anode side of the membrane is calculated from its definition, $a_w = p_w/p^*_w$, once the mole fraction of water and the partial pressure is determined. According to the assumption of constant chemical potential for water across the surface, this value is then also equal to the activity on the membrane side of the surface. From the activity, we can then calculate the water content on this side. At the cathode side of the membrane, we used $a^c_w = 1$ also across the

surface. The water activity in the membrane yields the corresponding water content in the membrane from eqs 82 and 83.

The fluxes of heat and charge (from eq 75) plus the transport coefficient (eqs 73, 78−81) and the water flux eq 83 are solved for the gradient in water activity in subsection 2.4. We replace $d\lambda_w/dx$ in eq 83 with $(d\lambda_w/da_w)(da_w/dx)$ and solve for da_w/dx.

Appendix D: Flux Equations for Electrode Surfaces

We give the flux equations to be solved for each of the electrode surfaces. The equations follow from the entropy production rate. The expression for σ^s (see subsections 2.3 and 2.5) has four terms, and it is necessary to introduce approximations for the coefficients. The surface is regarded as an excess resistance to transport. The most reasonable approximation is then to regard the resistances of the inside and of the outside as being in series. It follows that the coefficients that couple forces on different sides of the surface are zero in such a description.

We therefore write the forces as functions of fluxes for a system where heat and mass are transported in and out of the surface and electric current is transported through

$$\Delta_{i,s}\left(\frac{1}{T}\right) = r^s_{ii}J'^i_q + r^s_{i\mu}J^i_w + r^s_{io}J'^o_q + r^s_{im}J^o_w + r^s_{i\phi}j$$

$$-\frac{1}{T^s}\Delta_{i,s}\mu_{w,T} = r^s_{\mu i}J'^i_q + r^s_{\mu\mu}J^i_w + r^s_{\mu o}J'^o_q + r^s_{\mu m}J^o_w + r^s_{\mu\phi}j$$

$$\Delta_{s,o}\left(\frac{1}{T}\right) = r^s_{oi}J'^i_q + r^s_{o\mu}J^i_w + r^s_{oo}J'^o_q + r^s_{om}J^o_w + r^s_{o\phi}j$$

$$-\frac{1}{T^s}\Delta_{s,o}\mu_{w,T} = r^s_{mi}J'^i_q + r^s_{m\mu}J_w{}^i + r^s_{mo}J'^o_q + r^s_{mm}J^o_w + r^s_{m\phi}j$$

$$-\frac{1}{T^s}\Delta_{i,o}\phi_{eff} = r^s_{\phi i}J'^i_q + r^s_{\phi\mu}J^i_w + r^s_{\phi o}J'^o_q + r^s_{\phi m}J^o_w + r^s_{\phi\phi}j$$

The superscript i means into the surface, while o means out of the surface. There is a discontinuity in the heat flux at the surface, so we distinguish between the flux into the surface, J'^i_q, and out of the surface, J'^o_s. The same applies to the water flux at the surface. The driving force for charge transfer is the effective force as defined in subsections 2.3 and 2.5. The heat fluxes on the two sides obey the equation for energy conservation.

It is in this matrix that we now can assume that $r^s_{\mu o} = r^s_{o\mu} = 0$, $r^s_{\mu m} = r^s_{m\mu} = 0$, $r^s_{io} = r^s_{oi} = 0$, and $r^s_{im} = r^s_{mi} = 0$. It follows that we can write

$$J'^i_q = \frac{r^s_{\mu\mu}}{D^{i\mu}}\Delta_{i,s}\left(\frac{1}{T}\right) - \frac{r^s_{i\mu}}{D^{i\mu}}\left(-\frac{1}{T^s}\Delta_{i,s}\mu_{w,T}\right) + \pi^i\frac{j}{F}$$

$$J^i_w = -\frac{r_{\mu i}{}^s}{D^{i\mu}}\Delta_{i,s}\left(\frac{1}{T}\right) + \frac{r^s_{ii}}{D^{i\mu}}\left(-\frac{1}{T^s}\Delta_{i,s}\mu_{w,T}\right) + t^i\frac{j}{F}$$

$$J'^o_q = \frac{r^s_{mm}}{D^{om}}\Delta_{s,o}\left(\frac{1}{T}\right) - \frac{r^s_{om}}{D^{om}}\left(-\frac{1}{T^s}\Delta_{i,s}\mu_{w,T}\right) + \pi^o\frac{j}{F}$$

$$J^o_w = -\frac{r^s_{mo}}{D^{om}}\Delta_{s,o}\left(\frac{1}{T}\right) + \frac{r^s_{oo}}{D^{om}}\left(-\frac{1}{T^s}\Delta_{s,o}\mu_{w,T}\right) + t^o\frac{j}{F}$$

where

$$D^{i\mu} = r_{ii}r_{\mu\mu} - r_{i\mu}r_{\mu i}$$

$$D^{om} = r_{oo}r_{mm} - r_{om}r_{mo} \quad (84)$$

$$t^i_w = F\left(\frac{J^i_w}{j}\right)_{dT=0,d\mu=0} = F\frac{r_{i\phi}r_{\mu i} - r_{ii}r_{\mu\phi}}{D^{i\mu}}$$

$$t^o_w = F\left(\frac{J^o_w}{j}\right)_{dT=0,d\mu=0} = F\frac{r_{o\phi}r_{mo} - r_{oo}r_{m\phi}}{D^{om}} \quad (85)$$

$$\pi^i = F\left(\frac{J'^i_q}{j}\right)_{dT=0,d\mu=0} = F\frac{r_{\mu\phi}r_{\mu i} - r_{\mu\mu}r_{i\phi}}{D^{i\mu}}$$

$$\pi^o = F\left(\frac{J'^o_q}{j}\right)_{dT=0,d\mu=0} = F\frac{r_{m\phi}r_{mo} - r_{mm}r_{o\phi}}{D^{om}} \quad (86)$$

These coefficients are equal to the coefficients that were defined for the bulk phases. There is no coupling across the surface also in these equations. It follows that we can write the electric force the usual way

$$\Delta_{i,o}\phi_{eff} = -\frac{\pi^i}{T^iF}\Delta_{i,s}T - \frac{\pi^o}{T^oF}\Delta_{s,o}T - \frac{t^i_w}{F}\Delta_{i,s}\mu_{w,T} - \frac{t^o_w}{F}\Delta_{s,o}\mu_{w,T} - r^sj \quad (87)$$

where r^s is the (ohmic) surface resistivity.

In addition, we have the heats of transfer, from the linear relations

$$q^{*,i} = -\frac{r_{i\mu}}{r_{ii}} \quad (88)$$

$$q^{*,o} = -\frac{r_{om}}{r_{oo}} \quad (89)$$

By introducing these ratios, we obtain for each of the forces, which cover half of the surface

$$\Delta_{i,s}T = -\frac{J'^i_q}{\lambda^s_i} + \frac{q^{*,i}}{\lambda^s_i}\left(J^i_w - t^i_w\frac{j}{F}\right) + \pi^i\frac{j}{F\lambda^s_i} \quad (90)$$

$$\Delta_{i,s}\mu_{w,T} = -\frac{q^{*,i}}{T^i}\Delta_{i,s}T - \frac{\left(J^i_w - t^i_w\frac{j}{F}\right)}{l_{\mu\mu}} \quad (91)$$

$$\Delta_{s,o}T = -\frac{J'^o_q}{\lambda^s_o} + \frac{q^{*,o}}{\lambda^s_o}\left(J^o_w - t^o_w\frac{j}{F}\right) + \pi^o\frac{j}{F\lambda^s_o} \quad (92)$$

$$\Delta_{s,o}\mu_{w,T} = -\frac{q^{*,o}}{T^i}\Delta_{s,o}T - \frac{\left(J^o_w - t^o_w\frac{j}{F}\right)}{l_{mm}} \quad (93)$$

Here, λ^s_i and λ^s_o are stationary state thermal conductivities of the i and o sides of the surface, respectively, and $l_{\mu\mu}$ and l_{mm} are stationary state mass conductivities. These equations capture the most important phenomena at the electrode surfaces. It is interesting to see that they are completely analogous to their bulk counterparts.

The differences $\Delta_{i,s}\mu_{w,T}$ and $\Delta_{s,o}\mu_{w,T}$ are given by the difference in the entropy times the temperature across the side

of the surface in question. This difference is *not* zero when there is equilibrium for water across the surface.

References and Notes

(1) Weber, A. Z.; Newman, J. *Chem. Rev.* **2004**, *104*, 4679.
(2) Vie, P. J. S.; Kjelstrup, S. *Electrochim. Acta* **2003**, *204*, 295.
(3) Mench, M. M.; Burford, D.; Davies, T. W. In Situ Temperature Distribution Measurement in an Operating Polymer Electrolyte Fuel Cell. In *Proceedings of IMECE'03, 2003 ASME International Mechanical Engineering Congress and Exposition*, Washington, DC, Nov 16−21, 2003.
(4) Yang, H.; Prakash, J. *J. Electrochem. Soc.* **2004**, *151*, A1222.
(5) Janssen, G. J. M. *J. Electrochem. Soc.* **2001**, *148*, A1313.
(6) Kjelstrup, S.; Vie, P. J. S.; Bedeaux, D. In *Surface Chemistry and Electrochemistry of Membranes*; Sørensen, T. S., Ed.; Marcel Dekker: New York, 1999; pp 483−510.
(7) Kjelstrup, S.; Røsjorde, A. Local Entropy Production, Heat and Water Fluxes Out of A One-Dimensional Polymer Electrolyte Fuel Cell. In *Proceedings of the 16th ECOS Conference*, June 30−July 2, 2003; Houbak, N., Elmegaard, B., Qvale, B., Moran, M. J., Eds.; Department of Mechanical Engineering, Technical University of Denmark: Copenhagen, Denmark, 2003.
(8) Mazumder, S.; Cole, J. V. *J. Electrochem. Soc.* **2003**, *150*, A1503.
(9) Fuller, T.; Newman, J. *J. Electrochem. Soc.* **1993**, *140*, 1219.
(10) Okada, T. *J. New Mater. Eletrochem. Syst.* **2001**, 209.
(11) Thomas, K.; Newman, J. *J. Electrochem. Soc.* **2003**, *150*, A176.
(12) de Groot, S. R.; Mazur, P. *Non-Equilibrium Thermodynamics*; Dover: London, 1984.
(13) Bedeaux, D.; Albano, A. M.; Mazur, P. *Physica A* **1976**, *82*, 438.
(14) Albano, A. M.; Bedeaux, D. *Physica A* **1987**, *147*, 407.
(15) Bedeaux, D.; Kjelstrup Ratkje, S. *J. Electrochem. Soc.* **1996**, *136*, 767
(16) Bedeaux, D.; Kjelstrup, S. *J. Non-Equilib. Thermodyn.* **2000**, *25*, 161.
(17) Gibbs, J. W. *The Scientific Papers of J. W. Gibbs*; Dover: New York, 1961
(18) Springer, T. E.; Zawodzinski, T. A.; Gottesfeld, S. *J. Electrochem. Soc.* **1991**, *138*, 2334.
(19) Rubi, J. M.; Kjelstrup, S. *J. Phys. Chem. B* **2003**, *107*, 13471.
(20) Aylward, G. H.; Findlay, T. J. V. *SI Chemical Data*, 3rd ed.; Wiley: New York, 1994.
(21) Hansen, E. M.; Egner, E.; Kjelstrup, S. *Metall. and Mater. Trans. B* **1998**, *29*, 69.
(22) Ottøy, M. Mass and Heat Transfer in Ion-Exchange Membranes. Ph.D. Thesis, Department of Physical Chemistry, Norwegian University of Science and Technology, Trondheim, Norway, 1996.
(23) Kjelstrup Ratkje, S.; Ottøy, M.; Halseid, R.; Strømgård, M. *J. Membr. Sci.* **1995**, *107*, 219.
(24) Nguyen, P. T.; Berning, T.; Djilali, N. *J. Power Sources* **2004**, *130*, 149.
(25) Bedeaux, D.; Kjelstrup, S. *Chem. Eng. Sci*. **2004**, *59*, 109.